Critical decay at higher-order glass-transition singularities

2004 J. Phys.: Condens. Matter 16 S4807

(http://iopscience.iop.org/0953-8984/16/42/001)

INSTITUTE OF PHYSICS PUBLISHING JOURNAL OF PHYSICS: CONDENSED MATTER

J. Phys.: Condens. Matter **16** (2004) S4807–S4830 PII: S0953-8984(04)78457-X

Critical decay at higher-order glass-transition singularities

W Götze and M Sperl

Physik-Department, Technische Universität München, 85747 Garching, Germany

Received 29 March 2004
Published 8 October 2004
Online at stacks.iop.org/JPhysCM/16/S4807
doi:10.1088/0953-8984/16/42/001

Abstract

Within the mode-coupling theory for the evolution of structural relaxation in glass-forming systems, it is shown that the correlation functions for density fluctuations for states at A_3- and A_4-glass-transition singularities can be presented as an asymptotic series in increasing inverse powers of the logarithm of the time t: $\phi(t) - f \propto \sum_i g_i(x)$, where $g_n(x) = p_n(\ln x)/x^n$ with p_n denoting some polynomial and $x = \ln(t/t_0)$. The results are demonstrated for schematic models describing the system by solely one or two correlators and also for a colloid model with a square-well-interaction potential.

(Some figures in this article are in colour only in the electronic version)

1. Introduction

Upon compressing or cooling glass-forming liquids, there evolves a peculiar relaxation scenario called glassy dynamics. It is characterized by control-parameter sensitive correlation functions or spectra which are stretched over large intervals of time t or frequency ω, respectively. The so-called mode-coupling theory (MCT) of ideal glass transition has been proposed [1] as a mathematical model for glassy dynamics. The basic version of that theory describes the system by M correlation functions $\phi_q(t), q = 1, 2, \ldots, M$, which have the meaning of canonically defined auto-correlators of density fluctuations for wavevector moduli q chosen from a grid of M values. The theory deals with a closed set of coupled nonlinear equations of motion for the $\phi_q(t)$. The coupling coefficients in these equations are determined by the equilibrium structure factors, which are assumed to be known smooth functions of control parameters like temperature T or density ρ. The solution of the MCT equations describes a transition from an ergodic liquid state to a non-ergodic glass state if the control parameters pass critical values T_c or ρ_c, respectively. This transition is accompanied by the appearance of a dynamical scenario, whose qualitative features can be understood by asymptotic solution of the equations for long times and control parameters close to the critical values. The asymptotic formulae establish the universal features of the glassy dynamics described by MCT. On the basis of this understanding, one can construct schematic models. These are based on

equations of motion which have the same general form as those derived within the microscopic theory of liquids, but use the number M of correlators and the coupling coefficients as model parameters. Thereby, one gets simplified models whose results can be used for the analysis of data [2].

The ideal liquid–glass transition described by MCT is a fold bifurcation exhibited by the equations of motion. One can show that all singularities that are generically possible are of the cuspoid type [3, 4]. Using Arnol'd's notation [5], an A_l is a bifurcation which is equivalent to that for the roots of a real polynomial of degree l. Simple schematic models using only a single correlator also exhibit, in addition to the fold singularity, the cusp singularity A_3 and the swallowtail singularity A_4 [2]. The bifurcation dynamics near a higher-order glass-transition singularity A_l, $l \geqslant 3$, is utterly different from the one near the liquid–glass-transition singularity of type A_2. A major new feature is the appearance of logarithmic decay yielding to a much stronger stretching than known for the A_2-scenario [6]. The result for the correlators of $M = 1$ models has been worked out in a certain leading-order multiple-scaling-law limit [7]. These formulae have been used to fit dielectric-loss data of glassy polymer melts [8–11], thereby providing some hint that the MCT for higher-order singularities might be of relevance for understanding glassy dynamics.

Let us consider a system of spherical particles interacting via a steep repulsion potential characterized by a diameter parameter d, which is complemented by an attractive potential. The latter shall be characterized by an extension length Δ and an attraction-potential depth u_0. Such a system is specified conveniently by three control parameters: the packing fraction $\varphi = \rho\pi d^3/6$, the dimensionless attraction strength $\Gamma = u_0/(k_B T)$ or the dimensionless effective temperature $\theta = 1/\Gamma$, and the relative attraction width $\delta = \Delta/d$. If δ is sufficiently large, this potential is a caricature of a van der Waals interaction. One gets a decreasing Γ^c-versus-φ^c line of liquid–glass transitions in the Γ–φ plane of the thermodynamic states similar to what was first calculated within MCT for Lennard-Jones systems [12]. For $\Gamma = 0$, the mentioned line terminates at the critical packing fraction φ^c_{HSS} for the vitrification of the hard-sphere system. The decrease of φ^c with increasing Γ^c expresses the intuitive fact that cooling stabilizes the glass state. If δ is sufficiently small, however, there appear two new phenomena. First, for small Γ, the Γ^c-versus-φ^c line increases. Cooling stabilizes the liquid because bond formation creates inhomogeneities which favour fluidity. The new liquid state for $\varphi > \varphi^c_{HSS}$ exhibits a reentry phenomenon. Glassification occurs not only by increasing Γ, i.e., by cooling, but also by decreasing Γ, i.e., by heating. Second, the Γ^c-versus-φ^c line can consist of two branches that form a corner. The low-Γ-branch is terminated by the high-Γ-branch. The latter continues into the glass state as a glass–glass-transition line, which has an A_3-singularity as its endpoint. These two phenomena have been found by using Baxter's model for the structure factor as input to the MCT equations [13, 14]. In these calculations, the wavevector cutoff q_{max} used in the MCT model defines the range parameter $\delta = \pi/(q_{max}d)$. The generic possibility for a transition from small-δ states with A_3-singularity to large-δ states without A_3-singularity is the appearance of an A_4-singularity for some critical value δ^*. Since the A_l bifurcations deal with topological singularities, the indicated scenarios are robust, i.e., they occur for all potentials of the kind specified above. The A_4-singularity was identified first for the square-well system (SWS), i.e., for a system where a hard-core repulsion is complemented by a shell of constant attraction strength u_0. Here, $\delta^* \approx 0.04$ was calculated [15]. The neighbourhood of the A_4 was analysed for some other potentials with the conclusion that there are no qualitative differences between results referring to different shapes of the potential or to different approximation schemes for the structure factor [16].

The above-described systems with short-ranged attraction can be prepared as colloidal suspensions. The liquid–glass-transition lines can be identified by analysing the nucleation

processes. Light-scattering experiments can provide the density-correlation functions $\phi_q(t)$. Such studies have identified the existence of liquid states for $\varphi > \varphi^c_{HSS}$ and the reentry phenomenon [17–19]. Molecular-dynamics simulation studies can determine the mean-squared displacement and the diffusivities with good accuracy. These quantities exhibit drastic precursors of the liquid–glass transition. Several simulation studies [18, 20–22] have confirmed the predictions on the reentry phenomenon. Near the corner formed by the large-Γ and small-Γ transition lines, there should occur an almost logarithmic decay of the density correlations $\phi_q(t)$, which is followed by a von Schweidler-law decay as the beginning of an α-relaxation process [13, 15]. Such a scenario was first reported for micellar solutions [23]. This signature of the dynamics for $\varphi > \varphi^c_{HSS}$ states was also detected for colloidal suspensions with depletion attraction [19].

In order to identify a higher-order singularity in data from experiment or from molecular-dynamics simulation, one has to identify the features of the correlators $\phi_q(t)$ which are characteristic for these singularities. The general theory of the logarithmic decay laws caused by an A_l for $l \geqslant 3$ has been developed, and the relevant general scenarios have been illustrated for schematic models [24, 25]. The specific implications of the general theory for the SWS, in particular the change of the features with changes of the wavenumber and the peculiarities expected for the mean-squared displacement, have been worked out as well [26, 27]. Simulation data for the tagged-particle-density correlators as a function of the wavevector q [28] provide a first hint that the predicted logarithmic decay processes for $\varphi > \varphi^c_{HSS}$ states near an A_3-singularity are present. Major progress was reported recently for simulation studies for two states of a binary SWS [29]. The logarithmic decay and its expected deformation with wavenumber changes has been detected convincingly. The identified amplitudes agree semi-quantitatively with the calculated ones [26]. In addition, the mean-squared displacement exhibits the expected control-parameter dependent power-law behaviour. These findings provide very strong arguments for the existence of a higher-order glass-transition singularity. One concludes that the cited MCT results on simple systems with short-ranged attraction reproduce some subtle features of glassy dynamics so that further studies of these systems within that theory seem worthwhile.

If one shifts the control parameters towards those specifying a higher-order singularity, the time interval for logarithmic decay expands. But, simultaneously, the beginning of the time interval also shifts to larger values. Consequently, there opens a time interval of increasing length between the end of the transient and the beginning of the logarithmic decay. Within this interval, the correlators are close to the critical ones $\phi^c_q(t)$, i.e., to the correlators calculated for the control parameters at the singularity. It should be expected that these critical correlators will be detected in future data from experiments and from simulation studies. It was shown for one-component schematic models that the critical correlators approach their long-time limit proportional to $1/\ln^m(t/t_0)$, where $m = 2/(l-2)$ for an A_l [7]. In the following, these results shall be extended in two directions. First, the critical correlators shall be expanded in an asymptotic series so that an estimate of the range of validity of various asymptotic formulae is possible. Second, the $\phi^c_q(t)$ shall be calculated for the general theory so that a discussion of the q-dependent corrections of the leading asymptotic formulae is possible for an A_3- and an A_4-singularity.

The paper is organized as follows. In section 2, the general starting equations for an asymptotic discussion of critical relaxations are compiled. Then, in sections 3 and 4, the asymptotic expansion is carried out for one-component models for states near an A_3- and A_4-singularity, respectively. The results will be demonstrated quantitatively for schematic models. Section 5 shows how the theory for $\phi^c_q(t)$ for an A_3 can be reduced to the theory of one-component models. The results are demonstrated for a two-component schematic model

and for the SWS. The analogous results for an A_4-singularity are presented in section 6. A summary is formulated in section 7.

2. General equations

2.1. Equations for structural relaxation at glass-transition singularities

Within the basic version of the mode-coupling theory for the evolution of glassy relaxation (MCT), the system's dynamics is described by M correlators $\phi_q(t)$, $q = 1, \ldots, M$. The theory uses the exact Zwanzig–Mori equations of motion. These are specified by M characteristic frequencies $\Omega_q > 0$ and M fluctuating-force kernels $M_q(t)$. The latter are decomposed into regular terms $M_q^{\mathrm{reg}}(t)$ describing normal-liquid effects and in mode-coupling kernels $m_q(t)$. The essential step in the derivation of the theory is the application of Kawasaki's factorization approximation to express the kernels $m_q(t)$ as absolutely monotone functions $\mathcal{F}_q$ of the correlators. These functions depend smoothly on a vector $\mathbf{V}$ of control parameters like density and temperature,

$$m_q(t) = \mathcal{F}_q[\mathbf{V}, \phi_k(t)]. \tag{1}$$

Vector $\mathbf{V}$ specifies the equilibrium structure functions of the system. Using Laplace transforms of functions of time, say $F(t)$, to functions defined in the upper plane of complex frequencies z, $F(z) = \mathrm{i}\int_0^\infty \mathrm{d}t\, \exp(\mathrm{i}zt)F(t)$, the equations of motion read $\phi_q(z) = -1/\{z - \Omega_q^2[z + M_q^{\mathrm{reg}}(z) + \Omega_q^2 m_q(z)]\}$ [2]. Glassy dynamics is characterized by long-time decay processes that lead to large small-frequency contributions to $m_q(z)$. These small-z contributions to $m_q(z)$ dominate over $z + M_q^{\mathrm{reg}}(z)$. Therefore, glassy dynamics is described by the simplified equation $\phi_q(z) = -1/[z - 1/m_q(z)]$ [30]. Equivalently, there holds $\phi_q(z)/[1 - z\phi_q(z)] = m_q(z)$. It will be more convenient to modify the Laplace transform to another invertible mapping $\mathcal{S}$ from the time domain to the domain of complex frequencies according to

$$\mathcal{S}[F(t)](z) = (-\mathrm{i}z)\int_0^\infty \mathrm{d}t\ \exp(\mathrm{i}zt)F(t). \tag{2}$$

Using this notation, the MCT equations for the small-frequency dynamics read

$$\mathcal{S}[\phi_q(t)](z)/\{1 - \mathcal{S}[\phi_q(t)](z)\} = \mathcal{S}\left[\mathcal{F}_q[\mathbf{V}, \phi_k(t)]\right](z). \tag{3}$$

Since $\mathcal{F}_q$ is determined completely by the equilibrium structure functions, the dynamics obtained from equations (1) and (3) is referred to as structural relaxation. These equations are scale invariant: if $\phi_q(t)$ is a solution, the same is true for $\phi_q^x(t) = \phi_q(xt)$ for all $x > 0$. The scale for the dynamics is determined by the transient motion. The latter is governed by Ω_q and $M_q^{\mathrm{reg}}(t)$. Since these quantities do not enter equation (3), the solutions of equations (1) and (3) are fixed only up to an overall timescale [30]. In the following, this timescale will be denoted by t_0.

A glass state is characterized by non-vanishing long-time limits of the correlators: $\lim_{t\to\infty}\phi_q(t) = f_q, 0 < f_q < 1$. Equivalently, one gets $\lim_{z\to 0}\mathcal{S}[\phi_q(t)](z) = f_q$. Hence, the zero-frequency limit of equation (3) yields $f_q/(1 - f_q) = \mathcal{F}_q[\mathbf{V}, f_k]$, $q = 1, 2, \ldots, M$. This is a set of M implicit equations to be obeyed by the M numbers f_q [1]. If the Jacobian of these equations is invertible, the solutions vary smoothly with changes of $\mathbf{V}$. If the Jacobian is singular for some state $\mathbf{V}^{\mathrm{c}}$ with $f_q = f_q^{\mathrm{c}}$, f_q exhibits a singularity as a function of $\mathbf{V}$ for $\mathbf{V}$ tending towards $\mathbf{V}^{\mathrm{c}}$. Therefore, such a state $\mathbf{V}^{\mathrm{c}}$ is called a glass-transition singularity. The solution for the correlators for $\mathbf{V} = \mathbf{V}^{\mathrm{c}}$ is referred to as a critical correlator $\phi_q^{\mathrm{c}}(t)$. Let us introduce the functions $\hat{\phi}_q(t)$ by

$$\phi_q^{\mathrm{c}}(t) = f_q^{\mathrm{c}} + (1 - f_q^{\mathrm{c}})\hat{\phi}_q(t) \tag{4}$$

obeying $\lim_{t\to\infty}\hat{\phi}_q(t) = 0$. In the following, $\hat{\phi}_q(t)$ and $\mathcal{S}[\hat{\phi}_q(t)](z)$ shall be used as small quantities for an asymptotic expansion of $\phi_q^{\mathrm{c}}(t)$ for large times and small frequencies. Introducing the coefficients

$$A^{(n)c}_{qk_1\cdots k_n} = \frac{1}{n!}(1-f_q^{\mathrm{c}})\{\partial^n\mathcal{F}_q[\mathbf{V}^{\mathrm{c}}, f_k^{\mathrm{c}}]/\partial f_{k_1}\cdots\partial f_{k_n}\}(1-f_{k_1}^{\mathrm{c}})\cdots(1-f_{k_n}^{\mathrm{c}}), \tag{5}$$

equation (3) can be rewritten as the set of equations of motion for the $\hat{\phi}_q(t)$ [2]:

$$[\delta_{qk} - A^{(1)c}_{qk}]\mathcal{S}[\hat{\phi}_k(t)](z) = J_q(z). \tag{6}$$

Here, $J_q(z) = \sum_{n\geqslant 2} J_q^{(n)}(z)$ with the nth order expansion term given by

$$J_q^{(n)}(z) = A^{(n)c}_{qk_1\cdots k_n}\mathcal{S}[\hat{\phi}_{k_1}(t)\cdots\hat{\phi}_{k_n}(t)](z) - \mathcal{S}[\hat{\phi}_q(t)]^n(z). \tag{7}$$

In equations (6) and (7) and in all the following equations, summation over pairs of equal labels k is implied. The $M\times M$ matrix $[\delta_{qk} - A^{(1)c}_{qk}]$ is the Jacobian mentioned above. Therefore, a singularity is characterized by matrix $A^{(1)c}_{qk}$ to have an eigenvalue unity. It is a subtle property of the MCT equations that this eigenvalue is non-degenerate and that all other eigenvalues of $A^{(1)c}_{qk}$ have a modulus smaller than unity. The left and right eigenvectors shall be denoted by a_q^* and a_q, $q = 1,\ldots,M$, respectively:

$$a_k^* A^{(1)c}_{kq} = a_q^*, \qquad A^{(1)c}_{qk}a_k = a_q. \tag{8}$$

Generically, one can require $a_q \geqslant 0$, $a_q^* \geqslant 0$ for $q = 1,\ldots,M$. To fix the eigenvectors uniquely, two normalization conditions can be imposed: $\sum_q a_q^* a_q = 1$, $\sum_q a_q^* a_q a_q = 1$ [2, 3].

Because of the non-degeneracy mentioned, the singularity is topologically equivalent to that of the zeros of a real polynomial of degree l, $l = 2, 3, \ldots$. It is a bifurcation of type A_l [5]. The singularity can be characterized by a sequence of real coefficients $\mu_2, \mu_3, \ldots$. An A_l is specified by $\mu_n = 0$ for $n < l$ and $\mu_l \neq 0$. The simplest of these numbers reads

$$\mu_2 = 1 - \sum_q a_q^* A^{(2)c}_{qk_1k_2} a_{k_1}a_{k_2}. \tag{9}$$

For an A_2-glass-transition singularity, μ_2 determines the so-called critical exponent a, $0 < a \leqslant 1/2$. In this case, the critical correlator can be asymptotically expanded as a power series: $\hat{\phi}_q(t) = a_q(t_0/t)^a + a'_q(t_0/t)^{2a} + \cdots$. If the A_2 singularity approaches a higher-order singularity A_l, $l \geqslant 3$, the exponent a approaches zero and the cited asymptotic expansion breaks down [2]. It is the goal of this paper to derive a long-time expansion of the critical correlator at A_3- and A_4-singularities. Equivalently, it is the aim to solve asymptotically equations (6) and (7) for $\hat{\phi}_q(t)$ for states $\mathbf{V}^{\mathrm{c}}$ with

$$\mu_2 = 0, \qquad \mu_3 \neq 0 \tag{10a}$$

for an A_3-singularity denoted by $\mathbf{V} = \mathbf{V}^\circ$ and

$$\mu_2 = \mu_3 = 0, \qquad \mu_4 \neq 0 \tag{10b}$$

for an A_4-singularity denoted by $\mathbf{V} = \mathbf{V}^*$.

2.2. *Expansions of slowly-varying functions*

The derivations in this paper shall be based on an extension of the Tauberian theorem for slowly-varying functions, which has been introduced in [7]. A function $C(t)$ is called of slow variation for long times if $\lim_{T\to\infty} C(tT)/C(T) = 1$ for all $t > 0$. This is equivalent to $\gamma(z) = \mathcal{S}[C(t)](z)$ being slowly varying for small frequencies: $\lim_{T\to\infty}\gamma(z/T)/\gamma(\mathrm{i}/T) = 1$. In addition, the Tauberian theorem states that $\gamma(z)$ is asymptotically equal to

$G(\mathrm{i}/z) : \lim_{z\to 0} \gamma(z)/G(\mathrm{i}/z) = 1$ [31]. Typical examples for functions of slow variation are $p_m(\ln(\ln t))/\ln^m(t)$, where $m = 1, 2, \ldots$ and p_m denotes some polynomial. The critical correlator $\phi_q^c(t)$ shall be expressed as sum of such functions. Let us introduce the notations

$$G(t) = g(x), \qquad x = \ln(t/t_0), \qquad y = \ln(\mathrm{i}/zt_0), \tag{11a}$$

$$g_m(x) = p_m(x)/x^m, \qquad p_m(x) = \sum_{l=0}^{l_0} c_{m,l} x^l. \tag{11b}$$

$g_{m+1}(x)$ is asymptotically negligible compared to $g_m(x)$: $\lim_{x\to\infty} g_{m+1}(x)/g_m(x) = 0$. For later convenience, let us write $f(x) = \mathcal{O}(1/x^m)$ if $f(x)x^m$ is bounded for large x by some polynomial of $\ln x$. Denoting derivatives by $\mathrm{d}^n g(x)/\mathrm{d}x^n = g^{(n)}(x)$, $n = 0, 1, \ldots$, one finds

$$g_m^{(n)}(x) = \mathcal{O}(1/x^{m+n}). \tag{12}$$

Equation (2) can be rewritten as $\mathcal{S}[G(t)](z) = \int_0^\infty \exp(-u) g(y + \ln u)\, \mathrm{d}u$. Formal expansion in powers of $\ln u$ leads to

$$\mathcal{S}[G(t)](z) = \sum_{n=0}^{\infty} \frac{1}{n!} \Gamma_n g^{(n)}(y). \tag{13}$$

Here, $\Gamma_n = \Gamma^{(n)}(1)$ denotes the nth derivative of the gamma function at unity. One gets $\Gamma_0 = 1$, $-\Gamma_1 = \gamma$ is Euler's constant, and Γ_n for $n \geqslant 2$ can be expressed in terms of γ and Riemann's zeta-function values $\zeta(K)$ with $K = 2, \ldots, n$ [32]. For example, $\Gamma_2 - \Gamma_1^2 = \zeta(2)$. Using equation (13) with $G(t) = g_m(x)$, one gets an asymptotic expansion in terms of increasing order $\mathcal{O}(1/y^{m+n})$. The leading $n = 0$ contribution is $g_m(y)$; and this is the result of the Tauberian theorem [31]. The terms for $n \geqslant 1$ provide systematic improvements for large y, i.e., for large times or small frequencies [7].

If one uses equation (13) for $G(t) = G(t)F(t)$, one gets the asymptotic expansion

$$\mathcal{S}[G(t)F(t)](z) - \mathcal{S}[G(t)](z)\mathcal{S}[F(t)](z) = \sum_{n=2}^{\infty} \sum_{m=1}^{n-1} \frac{[\Gamma_n - \Gamma_{n-m}\Gamma_n]}{(n-m)!m!} g^{(n-m)}(y) f^{(m)}(y). \tag{14}$$

Let us use $G(t) = g_{m_1}(x)$ and $F(t) = g_{m_2}(x)$. The Tauberian theorem implies that the leading contribution to $\mathcal{S}[G_{m_1}(t)G_{m_2}(t)](z)$ cancels against the leading contribution to $\mathcal{S}[G_{m_1}(t)](z)\mathcal{S}[G_{m_2}(t)](z)$. The tricks underlying the asymptotic solution of the MCT equations at a higher-order singularity are based on the observation that the leading corrections to the Tauberian theorem also cancel [7]:

$$\mathcal{S}[g_{m_1}(t)g_{m_2}(t)](z) - \mathcal{S}[g_{m_1}(t)](z)\mathcal{S}[g_{m_2}(t)](z) = \mathcal{O}(1/y^{m_1+m_2+2}). \tag{15}$$

The difference between the two terms on the left-hand side is two orders smaller for vanishing frequencies than each of the terms separately.

3. Critical correlators for one-component models at an A_3-singularity

3.1. The leading contribution

It will be shown in section 5 how one can reduce the problem of solving equations (6) and (7) for a general number M of the correlators to the special problem of solving for $M = 1$ models. Therefore, the problem shall be discussed first for one-component models. For this case, one can drop the indices in all formulae of section 2.1. There is only one correlator $\phi^c(t)$, one long-time limit f^c for the critical point $\mathbf{V}^c$, and one function $\hat{\phi}(t)$ determining the critical

correlator as $\phi^c(t) = f^c + (1 - f^c)\hat{\phi}(t)$. The Jacobian matrix agrees with its eigenvalue, and this is zero. Hence, equations (6) and (7) can be noted as

$$K(z) = 0, \tag{16a}$$

$$K(z) = \sum_{n=2}^{\infty} K_n(z). \tag{16b}$$

Here, $K_n(z)$ is the expansion term of order $\hat{\phi}^n$. Let us introduce the abbreviation

$$\psi_n(z) = \mathcal{S}[\hat{\phi}^n(t)](z) - \mathcal{S}[\hat{\phi}(t)]^n(z), \tag{17}$$

and denote its inverse transform by $\psi_n(t)$, i.e., $\mathcal{S}[\psi_n(t)](z) = \psi_n(z)$. Remembering that for $M = 1$ models there holds $\mu_n = 1 - A^{(n)c}$, one gets $K_n(z) = \psi_n(z) - \mu_n \mathcal{S}[\hat{\phi}^n(t)](z)$ [24]. Specializing to the A_3-singularity as noted in equation (10*a*), the equation of motion (16*a*) is defined by

$$\begin{aligned} K(z) = {} & \psi_2(z) - \mu_3 \mathcal{S}[\hat{\phi}^3(t)](z) \\ & + \kappa\psi_3(z) - \mu_4 \mathcal{S}[\hat{\phi}^4(t)](z) \\ & + K'(z). \end{aligned} \tag{18}$$

Here, $K'(z) = \kappa'\psi_4(z) - \mu_5 \mathcal{S}[\hat{\phi}^5(t)](z) + \cdots$. The numbers κ and κ' have been introduced for later convenience. For the $M = 1$ models under consideration, one has to substitute $\kappa = \kappa' = 1$.

Let us examine whether one can solve the equations with the Ansatz $\hat{\phi}(t) = g_m(x) = c_m/x^m$. From equation (13) one gets $\mathcal{S}[\hat{\phi}^3(t)](z) = (c_m/y^m)^3 + \mathcal{O}(1/y^{3m+1})$. Using equation (14) with $G(t) = F(t) = g_m(x)$, one obtains $\psi_2(z) = \zeta(2)(mc_m/y^{m+1})^2 + \mathcal{O}(1/y^{2m+3})$. Choosing $m = 2$, both terms in the first line of equation (18) are of the same order $1/y^6$. They cancel in this leading order if $\mu_3 c_2^3 = 4\zeta(2)c_2^2$. From equations (13) and (15) one infers that the terms in the second line of equation (18) are of order $1/y^8$ and $K' = \mathcal{O}(1/y^{10})$. One concludes that the leading asymptotic behaviour of the critical correlator for large times is described by $\hat{\phi}(t) = g_2(x)$, where

$$g_2(x) = c_2/x^2, \qquad c_2 = 4\zeta(2)/\mu_3. \tag{19}$$

3.2. The leading correction

Let us split the function $\hat{\phi}(t)$ into its leading term and a correction $\tilde{g}(x)$:

$$\hat{\phi}(t) = g_2(x) + \tilde{g}(x). \tag{20}$$

Substitution of this formula into the first line of equation (18), one gets expressions up to third order in $\tilde{g}$. The term independent of $\tilde{g}$ is $\mathcal{S}[g_2^2(x)](z) - \mathcal{S}[g_2(x)]^2(z) - \mu_3 \mathcal{S}[g_2^3(x)](z)$, and it shall be denoted by $[(4\zeta(2))^2/\mu_3]F(y)$. Equations (13) and (14) are used to derive the asymptotic series

$$F(y) = \sum_{n=3}^{\infty} \frac{(-1)^{n+1}}{\mu_3 y^{4+n}} \left\{ \frac{1}{30}\zeta(2)\frac{(n+3)!}{(n-2)!}\Gamma_{n-2} - \sum_{m=1}^{n-2}(n-m+1)(m+1)(\Gamma_n - \Gamma_{n-m}\Gamma_m) \right\}. \tag{21a}$$

The term linear in $\tilde{g}$ is $2\{\mathcal{S}[g_2(x)\tilde{g}(x)](z) - \mathcal{S}[g_2(x)](z)\mathcal{S}[\tilde{g}(x)](z)\} - 3\mu_3 \mathcal{S}[g_2^2(x)\tilde{g}(x)](z)$. It shall be denoted by $[(4\zeta(2))^2/\mu_3][\mathcal{D}\tilde{g}(y) + \mathcal{D}'\tilde{g}(y)]$. Here, the differential operator $\mathcal{D}$ yields the leading contribution

$$\mathcal{D}\tilde{g}(y) = [y \cdot \mathrm{d}\tilde{g}(y)/\,\mathrm{d}y + 3\tilde{g}(y)]/y^4. \tag{21b}$$

The correction $\mathcal{D}'$ is expanded with the aid of equations (13) and (14):

$$\mathcal{D}'\tilde{g}(y) = [1/2\zeta(2)]\sum_{n=3}^{\infty}\sum_{m=1}^{n-1}(-1)^{n-m}\big\{[\tilde{g}^{(m)}(y)/y^{n+2-m}m!](\Gamma_n - \Gamma_{n-m}\Gamma_m) + \zeta(2)\Gamma_{n-2}$$
$$\times [\tilde{g}^{(m-1)}(y)/y^{n+3-m}(m-1)!](n-m+1)(n-m)(n-m+1)\big\}. \qquad (21c)$$

With these notations, the equation of motion for $\tilde{g}(y)$ is reformulated as a linear differential equation with some inhomogeneity $I(y)$:

$$\mathcal{D}\tilde{g}(y) = I(y), \qquad (22a)$$
$$I(y) = F(y) + \mathcal{D}'\tilde{g}(y) + \mathcal{S}[\tilde{g}^2(x)](z) - \mathcal{S}[\tilde{g}(x)]^2(z) - 3\mu_3\mathcal{S}[g_2(x)\tilde{g}^2(x)](z) - \mu_3\mathcal{S}[\tilde{g}^3(x)](z) + \kappa\psi_3(z) - \mu_4\mathcal{S}[\hat{\phi}^4(t)](z) + K'(z). \qquad (22b)$$

It might be adequate to emphasize that equations (19)–(22b) formulate an exact rewriting of equation (3) for $M = 1$ models.

The iterative solution of equation (22a) for $\tilde{g}(x)$ is based on the observation that one gets for functions $g_m(y)$ from equation (11b):

$$\mathcal{D}g_m(y) = [p'_m(y) + (3-m)p_m]/y^{m+4}. \qquad (23)$$

If one tries with $\tilde{g}(x) = g_3(x)$, one finds on the one hand $\mathcal{D}g_m(y) = p'_3(y)/y^7$. On the other hand, one verifies that all terms on the right-hand side of equation (22b) are $\mathcal{O}(1/y^8)$ except for the $n = 4$ contribution to $F(y)$. One checks that $F(y) = 24\zeta(3)/(\mu_3 y^7) + \mathcal{O}(1/y^8)$. Hence, the leading order solution for $\tilde{g}$ reads

$$g_3(x) = c_3\ln(x)/x^3, \qquad c_3 = 24\zeta(3)/\mu_3. \qquad (24)$$

Combining this finding with equations (19) and (20) and eliminating all the abbreviations, one reproduces a result of [7]:

$$\phi^\circ(t) = f^\circ + (1-f^\circ)[c_2/\ln^2(t/t_0)]\,\{1 + [6\zeta(3)/\zeta(2)]\ln\ln(t/t_0)/\ln(t/t_0)\}. \qquad (25)$$

This formula describes the critical correlator up to errors of the order $1/\ln^4(t/t_0)$.

3.3. Higher-order contributions

The equation for $\tilde{g}(y)$ allows for an iterative solution so that the iteration step with number m reads $\tilde{g} = g_3 + g_4 + \cdots + g_m$. Here the numerator polynomial in equation (11b) is of degree not larger than $(m-2)$, i.e.,

$$g_m(x) = \sum_{l=0}^{m-2} c_{m,l}\ln^l(x)/x^m. \qquad (26)$$

Suppose the procedure had been carried out up to step $m-1, m = 4, 5, \ldots$. Then $\mathcal{D}\tilde{g}(y) = \mathcal{D}g_m(y) + \mathcal{O}(1/y^{m+3})$. By construction, all terms up to order $(m+3)$ cancel against the one appearing in $I(y)$. One checks that the leading contribution to $I(y)$ reads $p(\ln y)/y^{m+4}$, where the degree of the polynomial p does not exceed $m-3$. Hence, equation (22a) is equivalent to the linear differential equation $p'_m + (3-m)p_m = p$. It is readily solved by equation (26), provided the coefficients $c_{m,l}$ are chosen properly.

In order to determine g_4 and g_5, one can drop $K'(z)$ in equation (22b). The coefficients $c_{m,l}$ are given by μ_3, κ, and μ_4 as follows:

$$c_{4,0} = 792\zeta(3)^2/(\pi^2\mu_3) + [4\mu_4/(9\mu_3^2) - 4\kappa/(3\mu_3) - 7/6]\pi^4/\mu_3, \qquad (27a)$$
$$c_{4,1} = -432\zeta(3)^2/(\pi^2\mu_3), \qquad (27b)$$
$$c_{4,2} = 648\zeta(3)^2/(\pi^2\mu_3), \qquad (27c)$$

$$c_{5,0} = \zeta(3)\pi^2[400\kappa\mu_3 + 1551\mu_3^2 - 160\mu_4]/(15\mu_3^3) - [39\,744\zeta(3)^3/\pi^4 + 528\zeta(5)]/\mu_3, \tag{28a}$$

$$c_{5,1} = 64\,800\zeta(3)^3/(\pi^4\mu_3) - 4\zeta(3)\pi^2(21\mu_3^2 - 24\kappa\mu_3 + 8\mu_4)/\mu_3^3, \tag{28b}$$

$$c_{5,2} = -27\,216\zeta(3)^3/(\pi^4\mu_3), \tag{28c}$$

$$c_{5,3} = 15\,552\zeta(3)^3/(\pi^4\mu_3). \tag{28d}$$

The coefficients for g_6 and g_7 have also been determined. The only new model parameters entering the coefficients are μ_5 and κ' [33].

3.4. Discussion

The preceding results shall be demonstrated quantitatively for the simplest model exhibiting a generic A_3-glass-transition singularity. This model was derived for a spin-glass system and it is defined by the mode-coupling function [34]

$$m(t) = v_1\phi(t) + v_3\phi^3(t). \tag{29}$$

Here, and in the following models, we use a Brownian short-time dynamics as specified by the equation of motion

$$\tau\partial_t\phi(t) + \phi(t) + \int_0^t \mathrm{d}t' m(t-t')\partial_t'\phi(t') = 0, \tag{30}$$

to be solved with the initial condition $\phi(t \to 0) = 1$. The short-time asymptote is $\phi(t) - 1 = -(t/\tau) + \mathcal{O}((t/\tau)^2)$. The singularity is obtained for the coupling constants $v_1^\circ = 9/8$ and $v_3^\circ = 27/8$. The critical long-time limit of the correlator is $f^\circ = 1/3$ [6, 24]. The other parameters entering the coefficients via equations (27) and (28) are $\mu_3 = 1/3$ and $\mu_4 = \mu_5 = \kappa = \kappa' = 1$. Thus, all expansion formulae are specified, except for the timescale t_0. To ease reference to various degrees of asymptotic expansions, let us introduce the abbreviation for the nth order approximation

$$\phi^\circ(t)_n = f^\circ + (1 - f^\circ)G_n(t), \qquad G_n(t) = \sum_{m=2}^{n} g_m(\ln(t/t_0)). \tag{31}$$

Figure 1 exhibits $\phi^\circ(t)$ as obtained from equations (29) and (30) for the state $\mathbf{V} = \mathbf{V}^\circ$. The approach to the critical plateau f° is significantly slower than the one for a typical A_2-singularity. In the latter case, the decay comes close to the plateau within a few decades of increase of the time when a deviation of 5% is used as a measure. Such a criterion is not met by the decay in figure 1 for the entire window in time shown. For $t = 10^{11}$, the critical correlator $\phi^\circ(t)$ is still 5.5% above f°. To apply the asymptotic approximation, one has to match the timescale t_0 at large times. A reliable determination of t_0 is not possible when using only $G_2(x)$ or $G_3(x)$. Using $G_7(x)$ and extending the numerical solution to $t/\tau = 10^{38}$, it is possible to fix $t_0/\tau = 1.6 \times 10^{-4}$. Notice that t_0 is several orders of magnitude smaller than the timescale τ for the transient dynamics. With this value for t_0, the successive asymptotic approximations are shown in figure 1. The leading approximation from equation (31), labelled G_2, deviates from the critical correlator strongly. Including the next-to-leading term $g_3(x)$ yields the approximation labelled G_3, i.e., equation (25). A square indicates that G_3 deviates from the critical correlator by less than 2% for $t/\tau \gtrsim 5 \times 10^5$. If that criterion is relaxed to 5%, G_3 obeys it for $t \gtrsim 10^3\tau$. The approximation by G_3 provides a first reasonable approximation to $\phi^\circ(t)$. Including further terms of the expansion improves the approximation as is shown for G_5 and G_7. One recognizes that proceeding from G_5 to G_7 still improves the range of applicability by one order of magnitude in time. We conclude that the asymptotic expansion explains quantitatively the critical decay at the A_3-singularity for all times outside the transient regime.

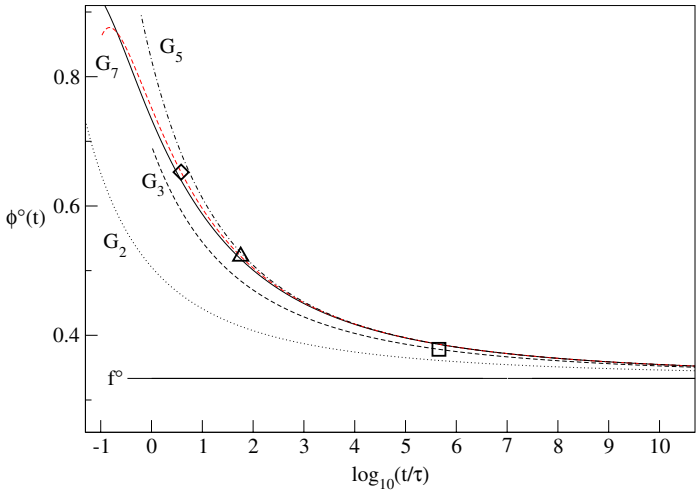

Figure 1. Critical decay at the A_3-singularity of the model defined by equations (29) and (30). The full curve shows the solution for $\phi^\circ(t)$. The curves labelled G_n, for $n = 2, 3, 5, 7$, show the approximations from equation (31) with the timescale $t_0/\tau = 1.6 \times 10^{-4}$. The time where G_3, G_5, and G_7 deviate by 2% from $\phi^\circ(t)$ is marked by a square (□), a triangle (△), and a diamond (◇), respectively.

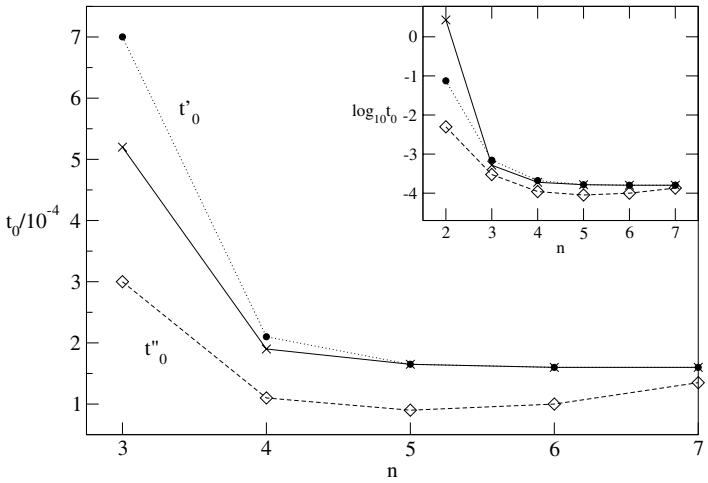

Figure 2. Timescale t_0 in units of τ for the approximation of the critical decay at the A_3-singularity of the model studied in figure 1 by including n orders of the asymptotic expansion, equation (31). Timescales obtained by matching $G_7(t)$ at large time, $35 \lesssim \log_{10} t \lesssim 38$, are shown by crosses (×). The times t_0' resulting from matching the solutions at $t = 10^6$ are shown by filled circles (•). The diamonds (◇) show the timescale t_0'' resulting from matching where $\phi(t) = 2/3$. The inset shows t_0 on a logarithmic scale. The lines are guides to the eye.

Matching a timescale t_0 at $t/\tau = 10^{38}$ and using six terms of the expansion in equation (31) is not a promising perspective for fitting data. However, the expansion leads to a reasonable approximation also for short times. Therefore, we may depart from the procedure to match t_0 at large times and try to fit t_0 for shorter times. Figure 2 shows as crosses the values obtained for t_0 when matching the approximations at the large times mentioned above. We will consider

two procedures for fitting. The first shall define a scale t_0' by matching the critical correlator by the approximation at $t = 10^6$. The second timescale t_0'' is obtained from matching at 50% of the decay, i.e., for the time t^* where $\phi^\circ(t^*) = 2/3$. We infer from the inset of figure 2 that all methods to fix t_0 based on the term $G_2(x)$ alone are off by orders of magnitude. The approximation $G_3(x)$ yields the correct order of magnitude for t_0 in all three approaches. Starting with $n = 5$, the scales t_0 and t_0' can no longer be distinguished. Therefore, matching the approximation at 10^6 is comparable to matching a true asymptotic limit. The value t_0' is a better approximation for t_0 than t_0''.

4. Critical correlators for one-component models at an A_4-singularity

Within the theory of the logarithmic decay as presented in [24], it is possible to specialize to the A_4-singularity by simply setting $\mu_3 = 0$ in the final formulae. Different from that, the critical decay for the A_4-singularity does not follow from the solution for the A_3-singularity but requires a different asymptotic expansion. This can be inferred from the fact that all the coefficients $c_{m,l}$ in equation (26) contain μ_3 in the denominator. However, the tricks used for finding a solution in terms of slowly varying functions are the same for the A_4 as explained above for the A_3.

4.1. The leading contribution

Using equation (10*b*) for an A_4-singularity, equations (16*a*) and (18) can be regrouped as

$$\begin{array}{rcccc} 0 = & & \psi_2(z) & - & \mu_4\,\mathcal{S}[\hat{\phi}^4(t)](z) \\ & + & \kappa\psi_3(z) & - & \mu_5\,\mathcal{S}[\hat{\phi}^5(t)](z) \\ & + & \kappa'\psi_4(z) & - & \mu_6\,\mathcal{S}[\hat{\phi}^6(t)](z) \\ & & & + & \ldots\ . \end{array} \tag{32}$$

With the Ansatz $\hat{\phi}(t) = g_m(x) = c_m/x^m$, one arrives for the terms of the first line at $\psi_2(z) = \zeta(2)(mc_m/y^{m+1})^2 + \mathcal{O}(1/y^{2m+3})$ and $\mathcal{S}[\hat{\phi}^4(t)](z) = (c_m/y^m)^4 + \mathcal{O}(1/y^{4m+1})$. For $m = 1$, the first line in equation (32) is of leading order $\mathcal{O}(1/y^4)$ with the equation for the coefficient $\zeta(2)c_1^2 = \mu_4 c_1^4$. This results in the leading-order solution [7],

$$g_1(x) = c_1/x, \qquad c_1 = \sqrt{\zeta(2)/\mu_4}. \tag{33}$$

4.2. The leading correction

The corrections may be rephrased in terms of a differential operator and the solution is straightforward as before. Since, later on, only the first correction will be needed explicitly, it will be calculated here by the linear differential equation for the Ansatz $\hat{\phi}(t) = [\phi^*(t) - f^*]/(1 - f^*) = g_1(x) + \tilde{g}(x)$,

$$2y^3\tilde{g}'(y) + 4y^2\tilde{g} = 4\sqrt{\zeta(2)/\mu_4}\zeta(3)/\zeta(2) + 3\zeta(2)\kappa/\mu_4 - \mu_5\zeta(2)/\mu_4^2. \tag{34}$$

This is solved in leading order by $g_2(x)$:

$$\begin{aligned} &g_2(x) = c_2\ln(x)/x^2, \\ &c_2 = 2\sqrt{\zeta(2)/\mu_4}\zeta(3)/\zeta(2) + 3\zeta(2)\kappa/(2\mu_4) - \mu_5\zeta(2)/(2\mu_4^2). \end{aligned} \tag{35}$$

Higher-order contributions for $m \geqslant 3$ can be written in the form

$$g_m(x) = \sum_{l=0}^{m-1} c_{m,l}\ln^l(x)/x^m \tag{36}$$

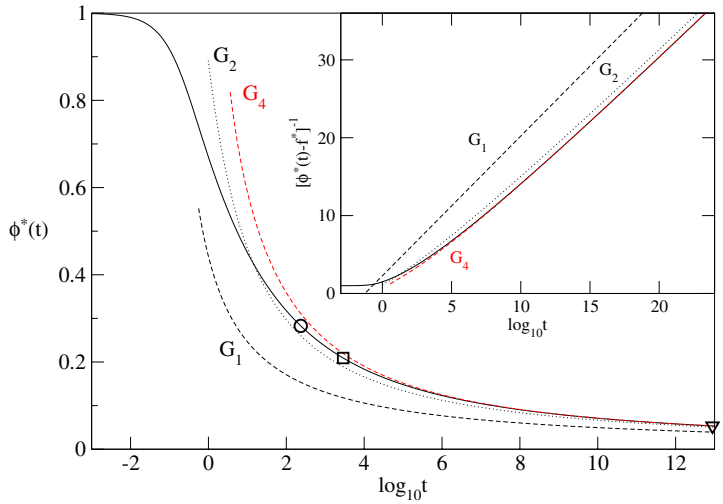

Figure 3. Critical decay $\phi^*(t)$ at the A_4-singularity of the model defined by equations (30) and (38), and the unit of time chosen such that $\tau = 1$. The approximations by equation (37) with $t_0 = 0.055$ matched for G_4 are labelled accordingly. The square and the circle mark the time where the approximation by G_4 deviates from the solution by 5% and 10%, respectively. The triangle refers to a 5% deviation of G_2 from the solution. The inset displays the inverse of $[\phi^*(t) - f^*]$ and its respective approximations.

with the appropriate choice of the parameters $c_{m,l}$. Hence, the general solution for the critical decay at an A_4-singularity in the one-component case is represented up to errors of order $\mathcal{O}(\ln^{-(n+1)}(t))$ as

$$\phi^*(t) = f^* + (1 - f^*)G_n(t), \qquad G_n(t) = \sum_{m=1}^{n} g_m(\ln(t/t_0)). \tag{37}$$

Because the leading order result $g_1(x)$ is of order $\mathcal{O}(1/\ln t)$ each higher-order solution requires the inclusion of an additional line in equation (32). This adds new parameters like μ_6 and κ' in each step, whereas for the A_3-singularity, equation (26), additional parameters occur only in every second step of the expansion.

4.3. Discussion

The results for the A_4-singularity shall be demonstrated for the kernel [6],

$$m(t) = v_1\phi(t) + v_2\phi^2(t) + v_3\phi^3(t), \tag{38}$$

substituted into the equation of motion (30) used with $\tau = 1$. The model has an A_4-singularity at $\mathbf{V}^* = (1, 1, 1)$ with $f^* = 0$ and coefficients $\mu_l, l \geqslant 4$ and κ being unity.

Using up to four terms in the expansion (37), the timescale is fixed at $t_0 = 0.055$. Successive approximations to the numerical solution are shown in figure 3. Again, the leading approximation G_1 does not describe the solution. The inset shows $[\phi^*(t) - f^*]^{-1}$, where a decay proportional to $1/\ln t$ would be seen as a straight line. G_1 yields such a straight line by definition; but it has the wrong slope compared to the solution. The latter exhibits a straight line for $t \gtrsim 10^7$. Including the leading correction in G_2 can account for the slope of the long-time solution. Further terms in the asymptotic expansion enhance the accuracy of the approximation. G_4 fulfills the 5% criterion at $t = 3 \times 10^3$, and is in accord with the solution

on the 10% level for $t > 230$. G_2 intersects $\phi^*(t)$ for shorter times but deviates first from the solution by 5% at $t = 9 \times 10^{12}$.

5. Asymptotic expansion of the critical correlators at an A_3-singularity

For the study of the general models, we go back to equations (4)–(7). The solvability condition for equation (6) reads

$$\sum_q a_q^* J_q(z) = 0, \tag{39a}$$

and the general solution can be written as

$$\hat{\phi}_q(t) = a_q \hat{\phi}(t) + \tilde{\phi}_q(t). \tag{39b}$$

The splitting of $\hat{\phi}_q(t)$ in two terms is unique if one imposes the convention $\sum_q a_q^* \hat{\phi}_q(t) = \hat{\phi}(t)$. Then, the part $\tilde{\phi}_q(t)$ can be expressed by means of the reduced resolvent R_{qk} of $A^{(1)c}_{qk}$:

$$\mathcal{S}[\tilde{\phi}_q(t)](z) = R_{qk} J_k(z). \tag{39c}$$

The matrix R_{qk} can be evaluated from matrix $A^{(1)c}_{qk}$ and the vectors a_k^*, a_k [35]. Let us emphasize that equations (39*a*)–(39*c*) together with the definitions in equations (4) and (7) are an exact reformulation of the equation of motion (3) for states at glass-transition singularities. It is the aim of following calculations to express $\tilde{\phi}_q(t)$ recursively in terms of $\hat{\phi}(t)$ and to show that $\hat{\phi}(t)$ has the asymptotic expansion discussed in section 3 for the one-component models. The starting point is the observation that $\tilde{\phi}_q(t)$ is small and of higher order than $\hat{\phi}(t)$. This is obvious, since equations (7) and (39*c*) imply $\tilde{\phi}_q(z) = \mathcal{O}(\hat{\phi}^2) + \mathcal{O}(\hat{\phi}\tilde{\phi}_q) + \mathcal{O}(\tilde{\phi}_q^2)$. Therefore, one gets

$$J_q(z) = \mathcal{O}(\hat{\phi}^2), \tag{40a}$$

$$\tilde{\phi}_q(t) = \mathcal{O}(\hat{\phi}^2). \tag{40b}$$

We assume that $\hat{\phi}$ can be expanded in terms of functions $g_m(x)$ as defined in equations (11*a*), (11*b*), and show the legitimacy of this Ansatz by the success of the following constructions.

5.1. Expansion up to next-to-leading order

Substituting the splitting (39*b*) into the inhomogeneity $J_q^{(2)}(z)$ from equation (7) yields

$$J_q(z) = A^{(2)c}_{qk_1k_2} a_{k_1} a_{k_2} \mathcal{S}[\hat{\phi}(t)^2](z) - a_q^2 \mathcal{S}[\hat{\phi}(t)]^2(z) + \mathcal{O}(\hat{\phi}^3). \tag{41}$$

The function $\psi_2(z)$ in equation (17) is of order $\mathcal{O}(\hat{\phi}^3)$ because of equation (15). Therefore,

$$J_q(z) = (A^{(2)c}_{qk_1k_2} a_{k_1} a_{k_2} - a_q^2) \mathcal{S}[\hat{\phi}(t)^2](z) + \mathcal{O}(\hat{\phi}^3). \tag{42}$$

Remembering equation (9) and the condition $\mu_2 = 0$, one notices that the solvability condition (39*a*) is fulfilled to order $\mathcal{O}(\hat{\phi}^2)$. Hence, equation (39*c*) yields

$$\tilde{\phi}_q(t) = X_q \hat{\phi}^2(t) + \mathcal{O}(\hat{\phi}^3) \tag{43}$$

with the abbreviation [24]

$$X_q = R_{qk} \left[A^{(2)c}_{kk_1k_2} a_{k_1} a_{k_2} - a_k^2 \right]. \tag{44}$$

The first step in the derivation of q-dependent corrections results in the extension of equation (39*b*):

$$\hat{\phi}_q(t) = a_q \hat{\phi}(t) + X_q \hat{\phi}^2(t) + \tilde{\phi}'_q(t), \tag{45a}$$

where

$$\tilde{\phi}'_q(t) = \mathcal{O}(\hat{\phi}^3). \tag{45b}$$

The next step is started by substituting the result (45*a*) into equation (7) for $J_q(z)$. Terms of order $\mathcal{O}(\hat{\phi}^2)$ vanish altogether as demonstrated above, and only $a_q^2\psi_2(z)$ and additional terms of order $\mathcal{O}(\hat{\phi}^3)$ are left from $J_q^{(2)}(z)$. Equation (17) is used to reduce products of $\mathcal{S}$-transforms to $\mathcal{S}$-transforms of products. The inhomogeneity assumes the form

$$J_q(z) = \mathcal{S}[\hat{\phi}(t)^3](z)\left[A^{(3)c}_{qk_1k_2k_3}a_{k_1}a_{k_2}a_{k_3} + 2(A^{(2)c}_{qk_1k_2}a_{k_1}X_{k_2} - a_q^2) - (a_q^3 + 2a_qX_q)\right] + a_q^2\psi_2(z) + \mathcal{O}(\hat{\phi}^4). \tag{46}$$

Let us introduce $\kappa = 2\zeta$ and μ_3 in agreement with [24]:

$$\zeta = \sum_q a_q^*\left[a_qX_q + a_q^3/2\right], \tag{47a}$$

$$\mu_3 = 2\zeta - \sum_q a_q^*\left[A^{(3)c}_{qk_1k_2k_3}a_{k_1}a_{k_2}a_{k_3} + 2A^{(2)c}_{qk_1k_2}a_{k_1}X_{k_2}\right]. \tag{47b}$$

Then, the solvability condition (39*a*) reads

$$0 = \psi_2(z) - \mu_3\mathcal{S}[\hat{\phi}(t)^3] + \mathcal{O}(\hat{\phi}^4). \tag{48}$$

This equation was discussed in section 3. The result is $\hat{\phi}(t) = g_2(x) + g_3(x) + \mathcal{O}(1/x^4)$ with the functions $g_2(x)$ and $g_3(x)$ specified in equations (19) and (24), respectively. From equation (43), one infers that $\tilde{\phi}_q(t) = \mathcal{O}(1/x^4)$. For the solution up to next-to-leading order, only the first term on the right-hand side of equation (45*a*) matters. However, the discussion of the solvability condition including the $X_q\hat{\phi}^2(t)$-term was necessary in order to fix the important number μ_3, which enters equation (48) and thereby the cited formulae for $g_2(x)$ and $g_3(x)$.

5.2. Higher-order expansions

After substitution of equation (45*a*) into equation (7) in order to extend the expansion of $J_q(z)$, one can use equation (39*c*) to determine $\tilde{\phi}'_q(t)$ up to errors of order $\mathcal{O}(\hat{\phi}^4)$. There appears a new amplitude Y_q as

$$Y_q = R_{qk}\left\{[A^{(3)c}_{kk_1k_2k_3}a_{k_1}a_{k_2}a_{k_3} - a_k^3] + 2[A^{(2)c}_{kk_1k_2}a_{k_1}X_{k_2} - a_kX_k] + \mu_3a_k^2\right\}. \tag{49}$$

To get the last term in the curly bracket, equation (48) was used to express the frequency dependence of $J_q(z)$ in equation (46) solely by $\mathcal{S}[\hat{\phi}(t)^3](z)$. After this second reduction step, one gets the extension of equation (45*a*):

$$\hat{\phi}_q(t) = a_q\hat{\phi}(t) + X_q\hat{\phi}^2(t) + Y_q\hat{\phi}^3(t) + \tilde{\phi}''_q(t), \tag{50a}$$

where

$$\tilde{\phi}''_q(t) = \mathcal{O}(\hat{\phi}^4). \tag{50b}$$

Here, the contribution proportional to Y_q has g_2^3 as the lowest-order term, and therefore it is of higher order than g_5. However, the calculation of the amplitude Y_q is a prerequisite to determine the parameter μ_4, which will be needed below.

To continue, we substitute equation (50*a*) into the solvability condition (39*a*). The same tricks as before are required to yield a definition of μ_4 which is consistent with the equations for the one-component case. Before adding new terms from the expansion of $J_q(z)$ in equation (7),

the remaining terms of order $\mathcal{O}(\hat{\phi}^5)$ in equation (46) shall be collected from the lines with $n \leqslant 3$. A new parameter is introduced to shorten notation,

$$\tilde{\kappa} = 2\sum_q a_q^* a_q X_q, \tag{51}$$

and the contribution to $J_q(z)$ so far is $\kappa\psi_3(z) - \tilde{\kappa}\mathcal{S}[\hat{\phi}]\psi_2(z)$. Equation (48) can be used to eliminate $\psi_2(z)$. With the assistance of equation (17), this contribution is reduced to $\kappa\psi_3(z) - \mu_3\tilde{\kappa}\mathcal{S}[\hat{\phi}^4] + \mathcal{O}(\hat{\phi}^5)$. Next, the term from equation (7) for $n = 4$ is added and the term with $\tilde{\kappa}$ is absorbed in the definition of μ_4. Then, the solvability condition reads

$$0 = \kappa\psi_3(z) - \mu_4\mathcal{S}[\hat{\phi}^4] + \mathcal{O}(\hat{\phi}^5), \tag{52}$$

where the definition for the remaining parameter μ_4 is

$$\mu_4 = \sum_q a_q^* \big\{[a_q^4 - A^{(4)c}_{qk_1k_2k_3k_4} a_{k_1}a_{k_2}a_{k_3}a_{k_4}] + 3[a_q^2 X_q - A^{(3)c}_{qk_1k_2k_3} a_{k_1}a_{k_2}X_{k_3}] + [X_q^2 - A^{(2)c}_{qk_1k_2} X_{k_1}X_{k_2}] + 2[a_q Y_q - A^{(2)c}_{qk_1k_2} a_{k_1} Y_{k_2}]\big\} + \tilde{\kappa}\mu_3. \tag{53}$$

After having defined all the necessary parameters, we see that the solution from section 3.3 for $\hat{\phi}(t)$ is consistent with the solution of the q-dependent case as formulated in equation (50*a*). Keeping only terms up to errors of order $(1/\ln t)^6$, one arrives at the asymptotic formula for the critical correlator at an A_3-singularity,

$$\phi_q^\circ(t) = f_q^\circ + h_q^\circ\big\{g_2(x) + g_3(x) + [g_4(x) + K_q^\circ g_2^2(x)] + [g_5(x) + 2K_q^\circ g_2(x)g_3(x)]\big\}, \tag{54a}$$

with

$$h_q^\circ = (1 - f_q^\circ)a_q, \qquad K_q^\circ = X_q/a_q. \tag{54b}$$

The first line of equation (54*a*) expresses the factorization theorem: $\phi_q^\circ(t) - f_q^\circ$ is a product of a first factor h_q°, which is independent of time, and a second factor $[g_2(x) + g_3(x)]$, which is independent of the correlator index q. Factorization is first violated in order $1/\ln^4 t$, and only the terms with the amplitudes K_q° are responsible for that. The expansion for $\phi_q^\circ(t)$ can be carried out up to order $1/\ln^5 t$ if μ_4 is known. The next order includes $g_6(x)$ and requires knowledge of the additional parameter μ_5.

5.3. Discussion

As a simple example for the demonstration of the preceding results, an $M = 2$ model shall be considered. The MCT equations for Brownian dynamics read, for $q = 1, 2$,

$$\tau_q\partial_t\phi_q(t) + \phi_q(t) + \int_0^t m_q(t - t')\partial_{t'}\phi_q(t')\,\mathrm{d}t' = 0, \tag{55a}$$

$$m_1(t) = v_1\phi_1^2(t) + v_2\phi_2^2(t), \tag{55b}$$

$$m_2(t) = v_3\phi_1(t)\phi_2(t). \tag{55c}$$

This is a schematic model for a symmetric molten salt [36]. The model has three control parameters, $\mathbf{V} = (v_1, v_2, v_3)$. The glass-transition singularities in this system can be evaluated analytically. There is an A_4-singularity at $v_3^* \approx 24.78$, and A_3-singularities occur for $v_3 > v_3^*$. To allow for a comparison with previous work [24], we set $\tau_1 = \tau_2 = 1$ and choose the A_3-singularity for $v_3^\circ = 45$.

Let us use the rescaled correlators $\hat{\phi}_q^\circ(t) = [\phi_q^\circ(t) - f_q^\circ]/h_q^\circ$ for the following considerations. The result in equation (54*a*) assumes the form $\hat{\phi}_q^\circ(t) = G_5(x) + K_q^\circ\tilde{G}_5(x)$,

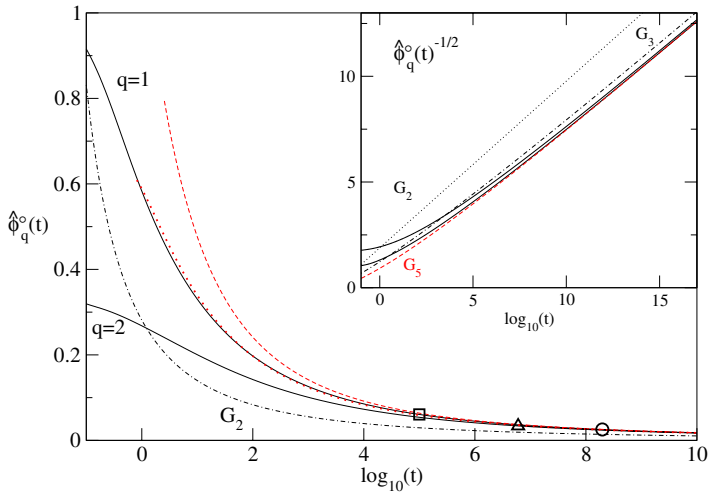

Figure 4. Critical decay at the A_3-singularity in the two-component model defined by equations (55*a*)–(55*c*) for $v_3^\circ = 45$ and $\tau_1 = \tau_2 = 1$. The rescaled solutions $\hat{\phi}_q^\circ(t) = [\phi_q^\circ(t) - f_q^\circ]/h_q^\circ$, $q = 1, 2$, are shown for as full curves. The asymptotic approximation (54*a*) is shown dashed for $q = 1$ and dotted for $q = 2$. The points where the approximation deviates by 5% from the solution for $q = 1, 2$, and the point where the solutions differ by 5% from each other are marked by a square, a triangle and a circle, respectively. The chain curve with label G_2 shows the leading contribution from equation (54*a*). The inset shows as full curves the rectification, $\hat{\phi}_q^\circ(t)^{-1/2}$ for $q = 1$ (lower full curve) and $q = 2$ (upper full curve). The q-independent part G_5 of the approximation in equation (54*a*) is given by the dashed curve. The dotted curve and the chain curve show the leading and next-to-leading order approximations G_2 and G_3, equation (54*a*). The timescale t_0 is 4.07×10^{-3}.

with $G_5(x)$ from equation (31) and $\tilde{G}_5(x) = g_2^2(x) + 2g_2(x)g_3(x)$. Since $\tilde{G}_5(x)$ is of higher order than $G_5(x)$, equation (19), correlators for different q approach each other for sufficiently large time as is demonstrated in figure 4. The time $t \approx 2 \times 10^8$, where $\hat{\phi}_2^\circ$ deviates by 5% from $\hat{\phi}_1^\circ$, is marked by a circle. The amplitude K_q° introduces the q-dependent corrections which are smaller for $q = 1$ than for $q = 2$. To evaluate $G_5(x)$ and $\tilde{G}_5(x)$, we determined the following parameters: $\mu_3 = 0.772$, $\kappa = 0.888$, and $\mu_4 = 1.38$. Notice that μ_3 is more than twice as big as for the model studied in figure 1. Since the coefficients $c_{m,l}$ in equation (26) contain powers of μ_3 in the denominator, corrections are smaller if μ_3 is larger; see equations (27*a*)–(27*c*) and (28*a*)–(28*d*). Because of the smaller corrections, the timescale can be matched with $G_5(x)$ between $t = 10^{20}$ and 10^{25}, which is significantly earlier than for the model studied in figure 1. We get $t_0 = 4.07 \times 10^{-3}$.

The asymptotic approximation (54*a*) is shown as a dashed curve for $q = 1$ in figure 4; it deviates by more than 5% from the solution if $t \lesssim 10^5$ (□). The approximation for $q = 2$ (dotted) deviates by more than 5% for $t \lesssim 6 \times 10^6$ (△). This difference in the range of validity can be understood qualitatively by considering the q-dependent corrections of higher order in equation (50*a*), $K_q[g_3^2(x) + 2g_2(x)g_4(x)] + Y_q g_2^3(x)/a_q$ with Y_q from equation (49). Both K_q and Y_q/a_q are smaller for the first correlator, $Y_1/a_1 = -0.1928$ and $Y_2/a_2 = 5.761$, and introduce fewer deviations from the q-independent part $G_6(x)$ of the approximation in higher order.

The q-independent function $G_5(x)$ would lie on top of the dashed curve in figure 4 and is therefore shown only in the inset, which also displays the critical correlators and the q-independent functions $G_2(x)$ and $G_3(x)$, equation (31). Plotting $\hat{\phi}_q^\circ(t)^{-1/2}$ we can

identify $1/\ln^2 t$-behaviour as a straight line. The critical correlators exhibit a straight line starting from $t \approx 10^9$. The leading approximation $G_2(x)$ is a straight line as well, but has a slope slightly larger than the solution. The first correction $G_3(x)$ resembles the slope of the solution but is offset from the solution by a shift of the timescale. This was observed before in figure 1. Since $G_5(x) + K_q^\circ \tilde{G}_5(x)$ was used to match the timescale t_0 and as $\tilde{G}_5(x)$ decays faster than the q-independent part, $G_5(x)$ coincides with the solution for larger times.

As a second example, the asymptotic laws shall be considered for the square-well system (SWS). This is the microscopic model for a colloid explained in section 1. The microscopic version of MCT for colloids is used with the wavevector moduli discretized to a set of $M = 500$ values. The structure factors that define the mode-coupling functional $\mathcal{F}_q$ in equation (1) are calculated in the mean-spherical approximation. We shall consider the same A_3-singularity for $\delta^\circ = 0.03$ as considered in previous studies [26, 27]. The reader is referred to these papers for further details and for an extensive discussion of the relaxation near the specified A_3-singularity. For the evaluation of the approximation (54*a*), we need the correction amplitudes K_q° which are shown in figure 8 of [26] and the parameters characteristic for the A_3-singularity under discussion,

$$\mu_3 = 0.109, \qquad \kappa = 0.314, \qquad \mu_4 = 0.204. \tag{56}$$

The asymptotic approximation reads

$$\begin{aligned}\hat{\phi}_q^\circ(t) = {} & 60.4/x^2 + 264.7 \ln x/x^3 \\ & + [3374.9 - 580.2 \ln x + 870.4 \ln^2 x]/x^4 \\ & + [-11\,745.7 - 27\,952.1 \ln x - 4452.2 \ln^2 x + 2544.1 \ln^3 x]/x^5 \\ & + K_q^\circ \left\{3643.9/x^4 + 31\,953.7 \ln x/x^5\right\} + \mathcal{O}(x^{-6}).\end{aligned} \tag{57}$$

The first line represents $g_2(x)$ and $g_3(x)$, equations (19) and (24). The second and third line exhibit the contributions up to $g_4(x)$ and $g_5(x)$, equations (26)–(28*d*), which are independent of the wavevector. The q-dependent correction terms appear with the prefactor K_q° in the curly brackets; they are positive for $t/t_0 > 2.5$ and monotonically decreasing for $t/t_0 > 3.1$.

Figure 5 shows the rescaled functions $\hat{\phi}_q^\circ(t)$ for three representative wavenumbers. At the peak of the structure factor, $qd = 7$, the amplitude is negative, for $qd = 57.4$ the correction amplitude is close to zero, and for the wavevector $qd = 172.2$ the amplitude is positive. The functions (full curves) deviate strongly from each other in the window of time presented, demonstrating severe violation of the factorization property. If the deviations among the correlation functions for different wavevectors cannot be assigned to the q-dependent corrections in equation (57) within an accessible window in time, we cannot expect that equation (57) will be sufficient to describe the critical decay. Suppose the critical correlators for different wavevectors are approximated by equation (57). Then, for arbitrarily chosen wavevectors q_1 and q_2, the difference $\hat{\Delta}[q_1, q_2](t) = \hat{\phi}_{q_1}^\circ(t) - \hat{\phi}_{q_2}^\circ(t)$ is given in leading order by the difference in the correction amplitudes, $K_{q_1}^\circ - K_{q_2}^\circ$, and the terms in the curly brackets in equation (57). From figure 5 we infer that $\hat{\Delta}[q_1, q_2](t)$ is not yet close enough to zero to neglect the terms in the curly brackets. The values of $\hat{\phi}_q^\circ(t)$ for the three chosen q-values are marked by diamonds in figure 5 for $t = 10^5$ and 10^{12}. We get $\hat{\Delta}[7, 57.4](10^5) = -0.030$ and $\hat{\Delta}[172.2, 57.4](10^5) = 0.161$. These differences are large but they correctly reflect the ordering in the values for K_q° which increase with q. From that we conclude that the treatment of the q-dependence in equation (57) is qualitatively correct.

If the time dependence of $\hat{\Delta}[q_1, q_2](t)$ were given exclusively by the terms in curly brackets in equation (57), then the differences among the K_q° would explain the amplitudes of the decay

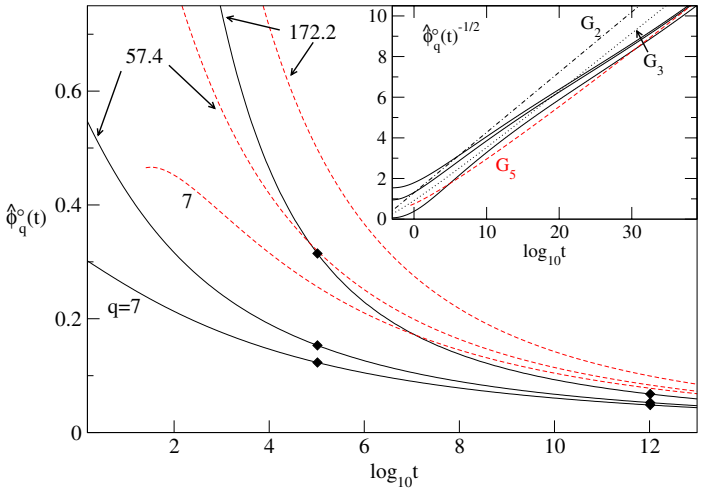

Figure 5. Critical decay at the A_3-singularity of the square-well system (SWS) for the relative attraction-shell width $\delta^\circ = 0.03$. Full curves show the rescaled correlation functions $\hat{\phi}_q^\circ(t) = [\phi_q^\circ(t) - f_q^\circ]/h_q^\circ$ at $\mathbf{V}^\circ$, for the wavevector values $qd = 7$, 57.4, and 172.2 as indicated. The unit of time is chosen so that $1/D_0 = 160$, with D_0 denoting the single particle diffusivity [26, 27]. The dashed curves exhibit the asymptotic approximation of equation (57) with a timescale $t_0 = 4\times10^{-5}$ matched in the interval $t = 10^{40}\cdots10^{45}$. For $qd = 7.0$, 57.4, and $qd = 172.2$, the correction amplitudes are $K_q^\circ = -1.704$, $-0.002\,24$, and 4.814, respectively. The filled diamonds for $t = 10^5$ and $t = 10^{12}$ mark the values for $\hat{\phi}_q^\circ(t)$ for the three q-values. The inset shows $\hat{\phi}_q^\circ(t)^{-1/2}$ for the q-values above from top to bottom and the q-independent approximations defined in equation (31) in the same representation, $G_2(t)^{-1/2}$, $G_3(t)^{-1/2}$ and $G_5(t)^{-1/2}$, respectively.

in $\hat{\Delta}[q_1, q_2](t)$. To quantify deviations from that case we introduce the ratio $\nu[q_1, q_2, q_3](t) = \hat{\Delta}[q_1, q_2](t)/\hat{\Delta}[q_2, q_3](t)$. For $t \to \infty$ this ratio is $\nu_\infty = (K_{q_1}^\circ - K_{q_2}^\circ)/(K_{q_2}^\circ - K_{q_3}^\circ)$. Deviations from ν_∞ indicate that higher-order q-dependent corrections are present in addition to the terms in equation (57). For the q-values used in figure 5 we get $\nu_\infty = (K_7^\circ - K_{57.4}^\circ)/(K_{57.4}^\circ - K_{172.2}^\circ) = 0.354$. Since $K_{57.4}^\circ \approx 0$, this ratio is almost equivalent to $-K_7^\circ/K_{172.2}^\circ$. The ratio at time $t = 10^5$ is $\nu[7, 57.4, 172.2](10^5) = 0.187$ and therefore deviates by 90% from ν_∞. Hence, we cannot expect equation (57) to describe the critical decay in figure 5 at that time. At $t = 10^{12}$, the ratio has decayed to $\nu[7, 57.4, 172.2](10^{12}) = 0.280$, which deviates from ν_∞ by 20%. Here, the q-dependent corrections are also in reasonable quantitative agreement with the approximation in equation (57). To determine t_0, we use extremely large times. The inset of figure 5 displays the rescaled correlators as $\hat{\phi}_q^\circ(t)^{-1/2}$. In this representation, the leading term $g_2(x)$ in equation (57) yields a straight line. We see that for large times the correlators for different q indeed come closer together, and the ratio at $t = 10^{40}$ is $\nu[7, 57.4, 172.2](10^{40}) = 0.341$, which deviates by 4% from ν_∞. For the determination of t_0 we use equation (57) for $q = 7$, 57.4, and 172.2 and match the asymptotic approximation to the numerical solutions in the interval from $t = 10^{40}$ to 10^{45}. This results in a value $t_0 = 4 \times 10^{-5}$. For times larger than $t \approx 10^{50}$ the numerical solution no longer follows the approximation. In that region inaccuracies in the control-parameter values lead to deviations from the asymptotic behaviour. These inaccuracies also prevent us from fixing more than just one digit of t_0. The dashed curve in the inset labelled G_5 shows the result for neglecting the last line of equation (57). This also describes the correlator for $q = 57.4$ where K_q is close to zero. Taking into account only the first line of equation (57) yields the dotted curve labelled G_3. This curve is clearly inferior to G_5, but it captures the slope of the solution still better than G_2.

In the large panel of figure 5, one can compare the critical correlators with the approximation by equation (57). For times of interest for experimental studies, the description is reasonable qualitatively. Especially the leading q-dependent corrections describe the variations seen in the correlators down to relatively short times. The accuracy of the approximation that was demonstrated for the schematic models in figures 4 and 1 is far better than seen in figure 5 for the SWS. This difference is mainly due to different values of the parameter μ_3 that characterizes the various A_3-singularities. For the two-component model we had $\mu_3 = 0.77$ and for the one-component model there was $\mu_3 = 1/3$. The small value $\mu_3 = 0.109$ for the SWS implies slow convergence of the asymptotic expansion. Therefore, a quantitative description by equation (57) is possible only for times exceeding considerably the ones shown in figure 5.

6. Asymptotic expansion of the critical correlators at an A_4-singularity

6.1. Expansion up to next-to-leading order

The calculation of the critical correlator at the A_4-singularity is so involved that we restrict ourselves to the leading and next-to-leading order result. The equations (40*a*)–(53) remain valid, and equations (49) and (53) simplify because $\mu_3 = 0$. The difficulty comes about because μ_5, which enters equation (35), has to be determined. This requires the extension of equation (50*a*), and thereby there appears a further amplitude. The additional amplitude Z_q is obtained by also including terms with $n = 4$ from equation (7). Applying the same manipulations as above, one arrives at $\tilde{\phi}_q''(t) = Z_q\hat{\phi}^4 + \mathcal{O}(\hat{\phi}^5)$ with the amplitude

$$\begin{aligned} Z_q = R_{qk}\big\{&[A^{(4)c}_{kk_1k_2k_3k_4}a_{k_1}a_{k_2}a_{k_3}a_{k_4} - a_k^4] + 3[A^{(3)c}_{kk_1k_2k_3}a_{k_1}a_{k_2}X_{k_3} - a_k^2X_k] \\ &+ [A^{(2)c}_{kk_1k_2}X_{k_1}X_{k_2} - X_k^2] + 2[A^{(2)c}_{kk_1k_2}a_{k_1}Y_{k_2} - a_kY_k] + \mu_4a_k^2\big\}. \end{aligned} \tag{58}$$

Introducing the third q-dependent correction, the solution assumes the form

$$\hat{\phi}_q(t) = a_q\hat{\phi}(t) + X_q\hat{\phi}^2(t) + Y_q\hat{\phi}^3(t) + Z_q\hat{\phi}^4(t) + \mathcal{O}(\hat{\phi}^5). \tag{59}$$

Collecting all terms of order $\mathcal{O}(\hat{\phi}^4)$ after including also the line $n = 5$ from equation (7), one gets from the solvability condition (39*a*):

$$\begin{aligned} \mu_5 = \sum_q a_q^*\big\{&[a_k^5 - A^{(5)c}_{kk_1k_2k_3k_4k_5}a_{k_1}a_{k_2}a_{k_3}a_{k_4}a_{k_5}] \\ &+ 4[a_k^3X_k - A^{(4)c}_{kk_1k_2k_3k_4}a_{k_1}a_{k_2}a_{k_3}X_{k_4}] \\ &+ 3[a_kX_k^2 + a_k^2Y_k - A^{(3)c}_{kk_1k_2k_3}(a_{k_1}X_{k_2}X_{k_3} + a_{k_1}a_{k_2}Y_{k_3})] \\ &+ 2[X_kY_k + a_kZ_k - A^{(2)c}_{kk_1k_2}(X_{k_1}Y_{k_2} + a_{k_1}Z_{k_2})]\big\} + \tilde{\kappa}\mu_4. \end{aligned} \tag{60}$$

Summarizing, the asymptotic solution for the critical decay at an A_4-singularity in next-to-leading order reads

$$\phi_q^*(t) = f_q^* + h_q^*\left\{g_1(x) + [g_2(x) + K_q^*g_1^2(x)]\right\}. \tag{61}$$

Here, in analogy to equation (54*b*), the critical amplitude is $h_q^* = (1 - f_q^*)a_q$ and the correction amplitude is given by $K_q^* = X_q/a_q$. The factorization theorem is obeyed by the leading-order term only. Contrary to what was found in equation (54*a*) for the behaviour at the A_3-singularity, the leading correction term g_2 is already modified by the q-dependent term $K_q^*g_1^2(x)$ of the same order. The higher-order contributions enter the curly brackets in equation (61) as $g_3(x) + 2g_1(x)g_2(x)X_q/a_q + g_1^3(x)Y_q/a_q$ and $g_4(x) + g_2^2(x)X_q/a_q + 2g_1(x)g_3(x)X_q/a_q + 3g_1^2(x)g_2(x)Y_q/a_q + g_1^4(x)Z_q/a_q$. However, $g_3(x)$ requires the evaluation of the parameters μ_6 and κ'; $g_4(x)$ needs μ_7 and κ''.

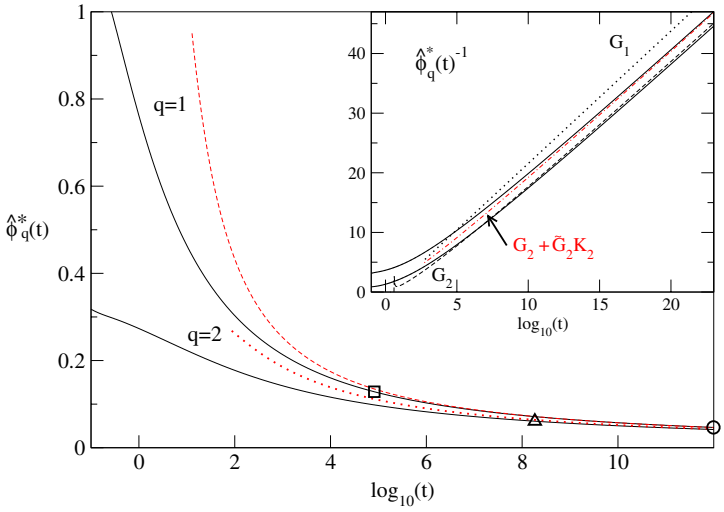

Figure 6. Rescaled critical decay $\hat{\phi}^*_q = [\phi^*_q(t) - f^*_q]/h^*_q$ at the A_4-singularity in the two-component model defined in equations (55*a*)–(55*c*) (full curves). The asymptotic approximations, equation (61), for $q = 1, 2$, are represented by the dashed and dotted curve, respectively. For $q = 1$ (□) and $q = 2$ (△), the points are marked where the solution and the approximation deviate by 5%. An additional point is indicated where the solution for $q = 2$ differs from the one for $q = 1$ by 10% (◯). The inset displays the rectified representation of the solutions for $q = 1$ (lower full curve) and $q = 2$ (upper full curve) together with the q-independent parts of the approximations, G_1 and G_2, cf equation (37), and $G_2 + K_2\tilde{G}_2$ (see text). The timescale $t_0 = 2.0$ was matched for $t = 10^{20} \cdots 10^{25}$.

6.2. *Discussion*

Figure 6 shows the critical decay at the A_4-singularity of the two-component model defined in equations (55*a*)–(55*c*). The parameters for the evaluation of $g_1(x)$ and $g_2(x)$ are $\mu_4 = 1.53$, $\mu_5 = 0.962$, and $\kappa = 0.386$. We use again the rescaled correlator $\hat{\phi}^*_q(t) = [\phi^*_q(t) - f^*_q]/h^*_q$ and check first the validity of the factorization in equation (61) in the form $\hat{\phi}^*_q(t) = G_2(x) + K_q\tilde{G}_2(x)$, where $G_2(x) = g_1(x) + g_2(x)$ and $\tilde{G}_2(x) = g_1^2(x)$. The time where the solutions for $q = 1, 2$ differ by 5% is only reached at $t \approx 10^{23}$. The circle marks the point where the deviation is still 10% at $t = 10^{12}$. We can then use the approximation (61) to fix the timescale to $t_0 = 2.0$, which then yields the dashed and dotted curves for $q = 1, 2$, accordingly. For $q = 1$ this approximation deviates by 5% from the solution at $t \approx 8.2 \times 10^4$ (□). For $q = 2$ we find $t \approx 1.8 \times 10^8$ (△). This is plausible when appealing to the q-dependent higher-order correction in equation (59), which also incorporates in addition to drastically different values for K_q the values $Y_1/a_1 = -0.579$ and $Y_2/a_2 = 3.76$. A rectified representation of the critical decay and the approximation in the inset again shows the leading-order $G_1(x)$ (dotted) as a straight line of different slope than the solution (full curves) and the second correction $G_2(x)$ (dashed). In this plot, the critical correlators for different q are still significantly different in the entire window. But equation (61) can account for that difference as is shown by the good agreement of the curve labelled $G_2 + \tilde{G}_2 K_2$. The latter describes the second correlator where the deviations due to the correction amplitudes are largest.

We now turn to the A_4-singularity of the SWS. For the application of equation (61) we need the parameters characterizing the A_4-singularity,

$$\mu_4 = 0.131, \qquad \kappa = 0.243, \qquad \mu_5 = 1.21. \tag{62}$$

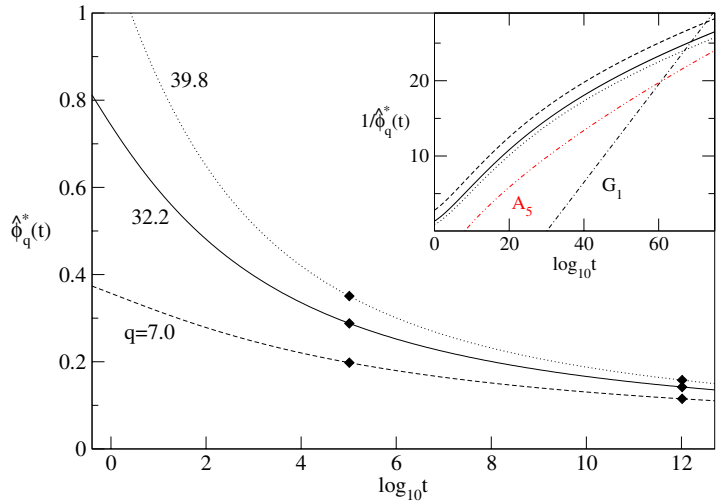

Figure 7. Critical decay at the A_4-singularity of the SWS for $qd = 7.0$ (dashed), 32.2 (full curve), 39.8 (dotted). The correction amplitudes are $K_q = -1.81$, -0.04, and 0.77, respectively. The filled diamonds mark the values at $t = 10^5$ and 10^{12} where the ratios $\nu(t)$ are 1.44 and 1.72, respectively (see text). The inset replots the curves from the full panel in the same linestyle and shows the first term of equation (63) labelled G_1 and the law $\ln(t/\tau)^{-2/3}$ labelled A_5, both with an arbitrary timescale.

The rather small value of μ_4 generates particularly large coefficients in the expansion of the critical decay in equation (36) where μ_4 appears in the denominators. This feature is quite the same as mentioned above for the A_3-singularities. The asymptotic approximation in equation (61) yields for the critical decay of the rescaled correlators

$$\hat{\phi}^*_q(t) = 3.54/x - 50.7 \ln x/x^2 + 12.5 K^*_q/x^2 + \mathcal{O}(x^{-3}). \tag{63}$$

We again choose values for q where K^*_q is negative, almost zero and positive. Figure 7 demonstrates that the factorization is strongly violated. Comparing the solutions $\hat{\phi}^*_q(t)$ for $t = 10^5$ we find a ratio defined as in the previous section of $\nu[7, 32.2, 39.8](10^5) = 1.439$ which is more than 30% off the ratio for the correction amplitudes $\nu_\infty = 2.185$. At $t = 10^{12}$ we find $\nu[7, 32.2, 39.8](10^{12}) = 1.723$, which achieves 20% accuracy. So the critical decay at the A_4-singularity shown in figure 7 is in qualitative accord with equation (63) with respect to the variation in q. However, due to the small value of μ_4, the differences among the correlators for different q do not decay fast enough to allow for a consistent determination of t_0 for the maximum value in time that could be reached. Numerically we find $\nu[7, 32.2, 39.8](10^{128}) = 2.076$, which is still 5% off from ν_∞, and $\hat{\phi}^*_q(t)$ itself deviates from zero by 5%. This illustrates drastically the enormous stretching at the A_4-singularity.

The inset of figure 7 demonstrates that the critical decay $\hat{\phi}^*_q(t)$ is qualitatively different from the leading order $1/\ln t$-law for $t \leqslant 10^{60}$. For the A_3-singularity in figure 5 it was still possible to argue that curve G_2 is in accord with the decay qualitatively at least for large times and to attribute deviations for shorter times to the proximity of the A_4-singularity. Figure 7 does not allow for such an interpretation. The curves $1/\hat{\phi}^*_q(t)$ have a slope smaller than $1/G_1$ over the complete window in time and imply a slower decay than given by the leading order in equation (63). If μ_4 was zero, the singularity would be of type A_5. The leading order critical decay at such a butterfly singularity is $\ln(t)^{-2/3}$. This law is added in the inset as a chain line labelled A_5. Indeed, it explains the data qualitatively. Hence, the

shortcomings of the asymptotic expansion at the A_4-singularity in the SWS result from the small value of μ_4.

To check if the value for μ_4 is exceptionally small for the SWS, the calculation was repeated for the hard-core Yukawa system as introduced in [16]. We find the even smaller value $\mu_4 = 0.080$. Therefore, the small value of μ_4 seems to be typical for systems with short-ranged attraction.

7. Summary

The asymptotic expansion for large times of the critical decay of correlation functions at higher-order glass-transition singularities has been elaborated. These decays can be considered as the analogue of the t^{-a}-law expansion for the correlators at the liquid–glass transition. The latter as well as the higher-order singularities are obtained as bifurcations of type A_l, $l \geqslant 2$. The A_l-singularity and especially the critical decay law at the singularity is characterized by a number μ_l. For the A_2-singularity of the liquid–glass transition, this characteristic number determines the so-called exponent parameter $\lambda = 1 - \mu_2$, which specifies the critical exponent a via $\lambda = \Gamma(1-a)^2/\Gamma(1-2a)$. For $\mu_2 = 0$ or $\lambda = 1$, one gets $a = 0$ and the asymptotic expansion in terms of powers t^{-a} becomes invalid. A higher-order singularity A_n is encountered, defined by $\mu_n > 0$ while $\mu_l = 0$ for $l < n$.

For an A_3-singularity, the critical decay is given by an expansion in inverse powers of the logarithm of the time, starting with $1/\ln^2 t$. The convergence of the asymptotic expansion is the better the larger is μ_3. The result for the general models in equations (54*a*) and (26) adds probing-variable dependent correction terms to the one-component result. These can be expressed by terms from the one-component solution and correction amplitudes. The leading correction amplitude K_q is the same function of the MCT-coupling constants as found earlier for the logarithmic decay-law expansions [24]. Since the vertex is a smooth function of the control parameters, these correction amplitudes are smooth functions as well. Therefore, also for the general case, the range of validity for the asymptotic expansion is determined by the characteristic parameter μ_3. If μ_3 is small, the quality of the fit by the asymptotic expansion is less satisfactory than for larger μ_3. Generically, larger μ_3 can be obtained by extending the corresponding glass–glass-transition line deeper into the glassy region and hence having the A_3-singularity further separated from the liquid regime. Thus, the dynamics influenced by an A_3-singularity seen in the liquid regime is either connected to a rather small μ_3, or it is strongly influenced by a crossing of different liquid–glass-transition lines [27].

For $\mu_3 = 0$, an A_4-singularity is found; the expansion for one-component models in equations (26)–(28*d*), (31) becomes invalid and has to be replaced by equations (36) and (37). The general solution in equation (61) has similar properties as mentioned above for the A_3-singularity. Now it is the characteristic parameter μ_4 that determines how satisfactory the approximation can be. While $\mu_4 = 1$ in figure 3 and $\mu_4 = 1.53$ in figure 6 allows for a description in the schematic models considered, the small parameter $\mu_4 \approx 0.1$ in the microscopic models for systems with short-ranged attraction prevents the application of the asymptotic formula.

An understanding of the critical decay law is a prerequisite for estimating the range of validity of the Vogel–Fulcher-type laws which describe the asymptotic limit of the timescale of the logarithmic decay laws near the higher-order singularities [7]. For the two-component model analysed above, the asymptotic limits were demonstrated for reasonable windows in time [25]. For the mentioned colloid models, the small values of the characteristic parameters μ_3 and μ_4 together with the manifest violation of the factorization property restrict such laws to unreasonably long times.

Acknowledgment

Our work was supported by the DFG Grant No. Go154/13-2.

References

[1] Bengtzelius U, Götze W and Sjölander A 1984 Dynamics of supercooled liquids and the glass transition *J. Phys. C: Solid State Phys.* **17** 5915–34

[2] Götze W 1991 Aspects of structural glass transitions *Liquids, Freezing and Glass Transition* (*Les Houches Summer Schools of Theoretical Physics* volume Session LI (1989)) ed J P Hansen, D Levesque and J Zinn-Justin (Amsterdam: North-Holland) pp 287–503

[3] Götze W and Sjögren L 1995 General properties of certain non-linear integro-differential equations *J. Math. Anal. Appl.* **195** 230–50

[4] Franosch T and Voigtmann Th 2002 Completely monotone solutions of the mode-coupling theory for mixtures *J. Stat. Phys.* **109** 237–59

[5] Arnol'd V I 1992 *Catastrophe Theory* 3rd edn (Berlin: Springer)

[6] Götze W and Haussmann R 1988 Further phase transition scenarios described by the self consistent current relaxation theory *Z. Phys.* B **72** 403–12

[7] Götze W and Sjögren L 1989 Logarithmic decay laws in glassy systems *J. Phys.: Condens. Matter* **1** 4203–22

[8] Sjögren L 1991 Dynamical scaling laws in polymers near the glass transition *J. Phys.: Condens. Matter* **3** 5023–45

[9] Flach S, Götze W and Sjögren L 1992 The *A*4 glass transition singularity *Z. Phys.* B **87** 29–42

[10] Halalay I C 1996 A mode-coupling theory catastrophe scenario description of relaxations in semicrystalline nylons *J. Phys.: Condens. Matter* **8** 6157–73

[11] Eliasson H 2001 Mode-coupling theory and polynomial fitting functions: a complex-plane representation of dielectric data on polymers *Phys. Rev.* E **64** 011802

[12] Bengtzelius U 1986 Theoretical calculations on liquid–glass transitions in Lennard-Jones systems *Phys. Rev.* A **33** 3433–9

[13] Fabbian L, Götze W, Sciortino F, Tartaglia P and Thiery F 1999 Ideal glass–glass transitions and logarithmic decay of correlations in a simple system *Phys. Rev.* E **59** R1347–50

Fabbian L, Götze W, Sciortino F, Tartaglia P and Thiery F 1999 Ideal glass–glass transitions and logarithmic decay of correlations in a simple system *Phys. Rev.* E **60** 2430

[14] Bergenholtz J and Fuchs M 1999 Non-ergodicity transitions in colloidal suspensions with attractive interactions *Phys. Rev.* E **59** 5706–15

[15] Dawson K, Foffi G, Fuchs M, Götze W, Sciortino F, Sperl M, Tartaglia P, Voigtmann Th and Zaccarelli E 2001 Higher order glass-transition singularities in colloidal systems with attractive interactions *Phys. Rev.* E **63** 011401

[16] Götze W and Sperl M 2003 Higher-order glass-transition singularities in systems with short-ranged attractive potentials *J. Phys.: Condens. Matter* **15** S869–79

[17] Eckert T and Bartsch E 2002 Re-entrant glass transition in a colloid–polymer mixture with depletion attractions *Phys. Rev. Lett.* **89** 125701

[18] Pham K N, Puertas A M, Bergenholtz J, Egelhaaf S U, Moussaïd A, Pusey P N, Schofield A B, Cates M E, Fuchs M and Poon W C K 2002 Multiple glassy states in a simple model system *Science* **296** 104–6

[19] Pham K N, Egelhaaf S U, Pusey P N and Poon W C K 2004 Glasses in hard spheres with short-range attraction *Phys. Rev.* E **69** 011503

[20] Foffi G, Dawson K A, Buldyrev S V, Sciortino F, Zaccarelli E and Tartaglia P 2002 Evidence for unusual dynamical arrest scenario in short ranged colloidal systems *Phys. Rev.* E **65** 050802

[21] Zaccarelli E, Foffi G, Dawson K A, Buldyrev S V, Sciortino F and Tartaglia P 2002 Confirmation of anomalous dynamical arrest in attractive colloids: a molecular dynamics study *Phys. Rev.* E **66** 041402

[22] Puertas A M, Fuchs M and Cates M E 2003 Simulation study of non-ergodicity transitions: gelation in colloidal systems with short range attractions *Phys. Rev.* E **67** 031406

[23] Mallamace F, Gambadauro P, Micali N, Tartaglia P, Liao C and Chen S-H 2000 Kinetic glass transition in a micellar system with short-range attractive interaction *Phys. Rev. Lett.* **84** 5431–4

[24] Götze W and Sperl M 2002 Logarithmic relaxation in glass-forming systems *Phys. Rev.* E **66** 011405

[25] Sperl M 2004 Logarithmic decay in a two-component model *Slow Dynamics in Complex Systems* (*AIP Conf. Proc.* vol 708) ed M Tokuyama and I Oppenheim (New York: American Institute of Physics)

[26] Sperl M 2003 Logarithmic relaxation in a colloidal system *Phys. Rev.* E **68** 031405
[27] Sperl M 2004 Dynamics in colloidal liquids near a crossing of glass- and gel-transition lines *Phys. Rev.* E **69** 011401
[28] Puertas A M, Fuchs M and Cates M E 2002 Comparative simulation study of colloidal gels and glasses *Phys. Rev. Lett.* **88** 098301
[29] Sciortino F, Tartaglia P and Zaccarelli E 2003 Evidence of a higher-order singularity in dense short-ranged attractive colloids *Phys. Rev. Lett.* **91** 268301
[30] Götze W and Sjögren L 1992 Relaxation processes in supercooled liquids *Rep. Prog. Phys.* **55** 241–376
[31] Feller W 1971 *An Introduction to Probability Theory and Its Applications* 2nd edn, vol II (New York: Wiley)
[32] Abramowitz M and Stegun I A 1970 *Handbook of Mathematical Functions* 7th edn (New York: Dover)
[33] Sperl M 2003 Asymptotic laws near higher-order glass-transition singularities *PhD Thesis* TU München
[34] Götze W and Sjögren L 1984 A dynamical treatment of the spin glass transition *J. Phys. C: Solid State Phys.* **17** 5759–84
[35] Gantmacher F R 1974 *The Theory of Matrices* vol II (New York: Chelsea)
[36] Bosse J and Krieger U 1987 Relaxation of a simple molten salt near the liquid–glass transition *J. Phys. C: Solid State Phys.* **19** L609–13